Supporting information

Effect of Structural Features on the Stability and Bactericidal Potential of Two Cadmium Coordination Polymers

Sajjad Soltani[1], Kamran Akhbari[1,*], Jonathan White[2]

[1]School of Chemistry, College of Science, University of Tehran, Tehran, Iran.

Tel.: +98 21 61113734; fax: +98 21 66495291.

E-mail address: akhbari.k@khayam.ut.ac.ir (K. Akhbari)

[2]School of Chemistry and Bio21 Institute, The University of Melbourne, VIC 3010, Australia

Table S1. Crystal data and structure refinement for compound $[Cd(Phac)_2(Dabco)(H_2O)]_n$ (**1**) and $[Cd(Phac)(4,4'\text{-Bpy})(OAc)]_n$ (**2**).

compound	**1**	**2**
Empirical formula	$C_{22}\ H_{28}\ Cd\ N_2\ O_5$	$C_{20}\ H_{18}\ Cd\ N_2\ O_4$
Formula weight	512.86	462.76
Temperature	100.0(2) K	100.0(2) K
Wavelength	0.710918Å	0.710913 Å
Crystal system	Orthorhombic	Triclinic
Space group	*P n m a*	$P\bar{1}$
Unit cell dimensions	a = 14.727(3) Å b =23.437(5) Å c = 5.9870(12) Å $\alpha = \beta = \gamma$ =90°	a = 9.3060(19) b =10.760(2) c =10.904(2) α = 114.49(3) β = 104.24(3) γ = 103.92(3)
Volume	2066.5(7) $Å^3$	887.5(4) $Å^3$
Z	4	2
Density (calculated)	1.648 $g.cm^{-3}$	1.732 $g.cm^{-3}$
Absorption coefficient	1.094 mm^{-1}	1.260 mm^{-1}
F(000)	1048	464
Theta range for data collection	2.766 to 32.416°.	2.2 to 32.2°.
Index ranges	$-18 \le h \le 18$ $-31 \le k \le 31$ $-8 \le l \le 8$	$-12 \le h \le 12$ $-14 \le k \le 14$ $-14 \le l \le 14$
Reflections collected	34660	16141
Independent reflections	3279 [R(int) = 0.0630]	4593 [R(int) =0.0384]
Data / restraints / parameters	3279 / 1 / 148	4593 / 0/ 246
Goodness-of-fit on F^2	1.113	1.114
Final R indices [I>2σ (I)]	R_1= 0.0461 wR_2= 0.1247	R_1=0.0361 wR_2=0.0997
R Indices (all data)	R_1= 0.0471 wR_2= 0.1255	0.0370 0.1005

Table S2. Selected bond lengths [Å] for **1** and **2**.

1	Bond lengths
O(1)-Cd(1)	2.338(2)
O(2)-Cd(1)	2.487(2)
O(3)-Cd(1)	2.252(3)
N(1)-Cd(1)	2.378(3)
N(2)-Cd(1)	2.401(3)

2	Bond lengths
N(1)-Cd(1)	2.324(2)
N(2)-Cd(1)	2.341(2)
O(3)-Cd(1)	2.363(2)
O(1)-Cd(1)	2.375(1)
O(1)-Cd(1)	2.382(2)
O(4)-Cd(1)	2.396(2)
O(2)-Cd(1)	2.476(2)
C(19)-Cd(1)	2.717(3)

Table S3. Selected angles [°] for **1** and **2**.

1	Angles	**2**	Angles
O(3)-Cd(1)-O(1)	133.66(6)	N(1)-Cd(1)-N(2)	169.19(8)
O(1)-Cd(1)-O(1)	91.78(11)	O(3)-Cd(1)-N(1)	89.75(8)
O(3)-Cd(1)-N(1)	96.20(10)	O(3)-Cd(1)-N(2)	87.85(8)
O(1)-Cd(1)-N(1)	101.30(6)	N(1)-Cd(1)-O(1)	96.49(7)
O(3)-Cd(1)-N(2)	88.11(10)	N(2)-Cd(1)-O(1)	91.90(7)
O(1)-Cd(1)-N(2)	86.26(6)	O(3)-Cd(1)-O(1)	141.72(7)
N(1)-Cd(1)-N(2)	175.70(9)	N(1)-Cd(1)-O(1)	90.46(8)
O(3)-Cd(1)-O(2)	80.26(6)	N(2)-Cd(1)-O(1)	86.20(8)
O(1)-Cd(1)-O(2)	53.88(8)	O(3)-Cd(1)-O(1)	149.03(7)
O(1)-Cd(1)-O(2)	145.66(8)	O(1)-Cd(1)-O(1)	68.91(8)
N(1)-Cd(1)-O(2)	90.25(4)	N(1)-Cd(1)-O(4)	97.50(9)
N(2)-Cd(1)-O(2)	90.49(4)	N(2)-Cd(1)-O(4)	89.80(9)
O(2)-Cd(1)-O(2)	160.45(12)	O(3)-Cd(1)-O(4)	55.33(7)
O(3)-Cd(1)-C(8)	106.79(6)	O(1)-Cd(1)-O(4)	86.39(7)
O(1)-Cd(1)-C(8)	27.06(8)	O(1)-Cd(1)-O(4)	154.79(7)
	118.82(9)	N(1)-Cd(1)-O(2)	82.60(8)
O(1)-Cd(1)-C(8)	91.38(5)	N(2)-Cd(1)-O(2)	87.14(8)
N(1)-Cd(1)-C(8)	87.37(5)	O(3)-Cd(1)-O(2)	95.53(7)
N(2)-Cd(1)-C(8)	26.84(10)	O(1)-Cd(1)-O(2)	122.70(7)
O(2)-Cd(1)-C(8)	172.55(8)	O(1)-Cd(1)-O(2)	53.86(6)
O(2)-Cd(1)-C(8)		O(4)-Cd(1)-O(2)	150.81(6)

Table S4. Hydrogen bonds for **1** [Å and °].

D-H...A	d(D-H)	d(H...A)	d(D...A)	<(DHA)
C(10)-H(10A)...O(1)#4	0.97	2.62	3.256(4)	123.0
C(10)-H(10B)...O(1)#2	0.97	2.62	3.256(4)	123.0
O(3)-H(3A)...O(1)#5	0.827(10)	1.926(17)	2.702(3)	156(3)
O(3)-H(3A)...O(2)	0.827(10)	2.94(4)	3.060(3)	91(3)
C(10)-H(10A)...O(1)#4	0.97	2.62	3.256(4)	123.0
C(10)-H(10B)...O(1)#2	0.97	2.62	3.256(4)	123.0
O(3)-H(3A)...O(1)#5	0.827(10)	1.926(17)	2.702(3)	156(3)
O(3)-H(3A)...O(2)	0.827(10)	2.94(4)	3.060(3)	91(3)

Symmetry transformations used to generate equivalent atoms:
#1 x,-y+1/2,z #2 x+1/2,y,-z+1/2 #3 x-1/2,y,-z+1/2
#4 x+1/2,-y+1/2,-z+1/2 #5 x,y,z-1

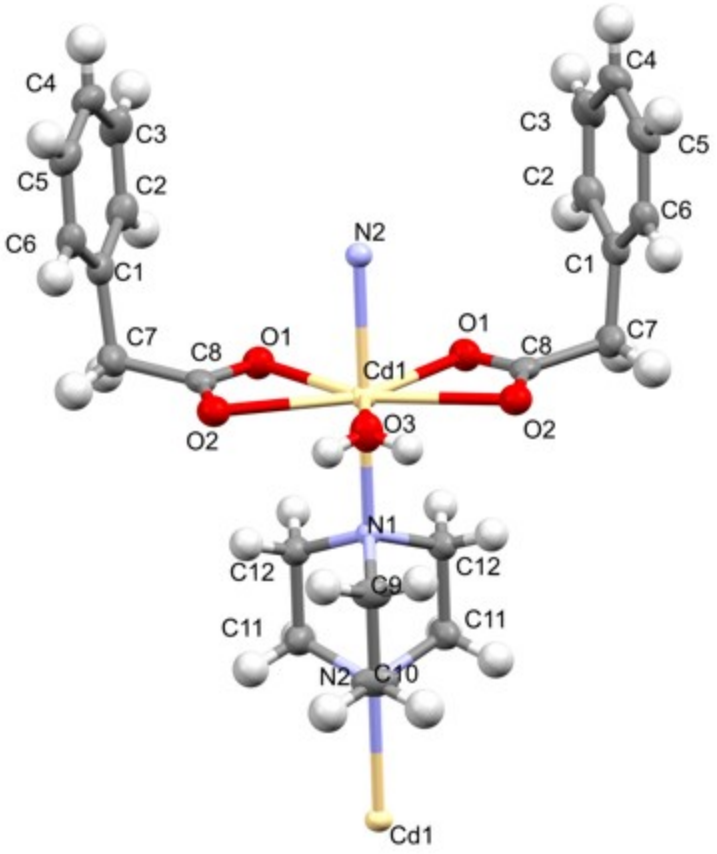

Figure S1. A thermal ellipsoid model of **1**. The thermal ellipsoids are set at a 50% probability level.

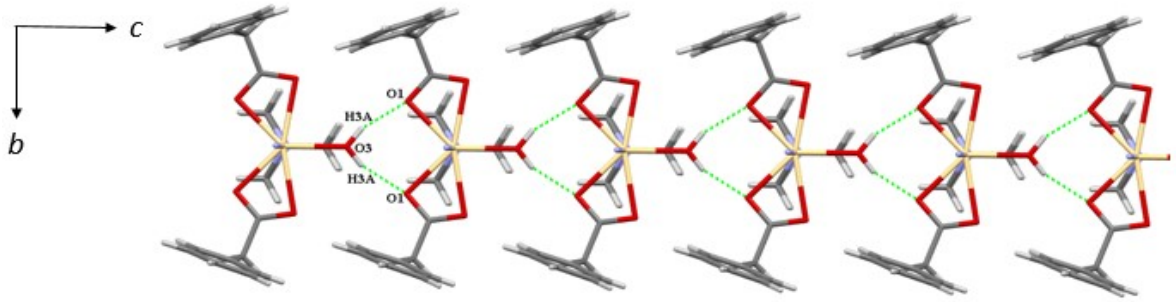

Figure S2. Expansion of 1 structure by hydrogen bonds.

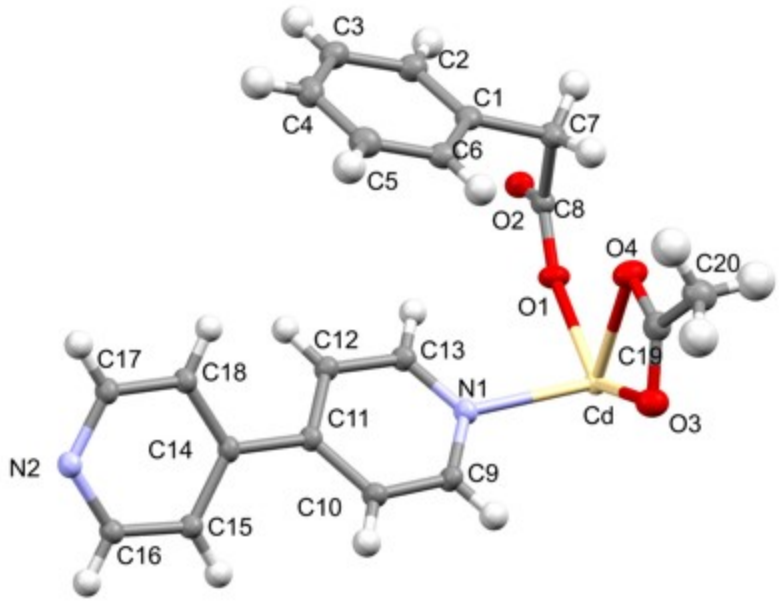

Figure S3. A thermal ellipsoid model of **2**. The thermal ellipsoids are set at a 50% probability level.

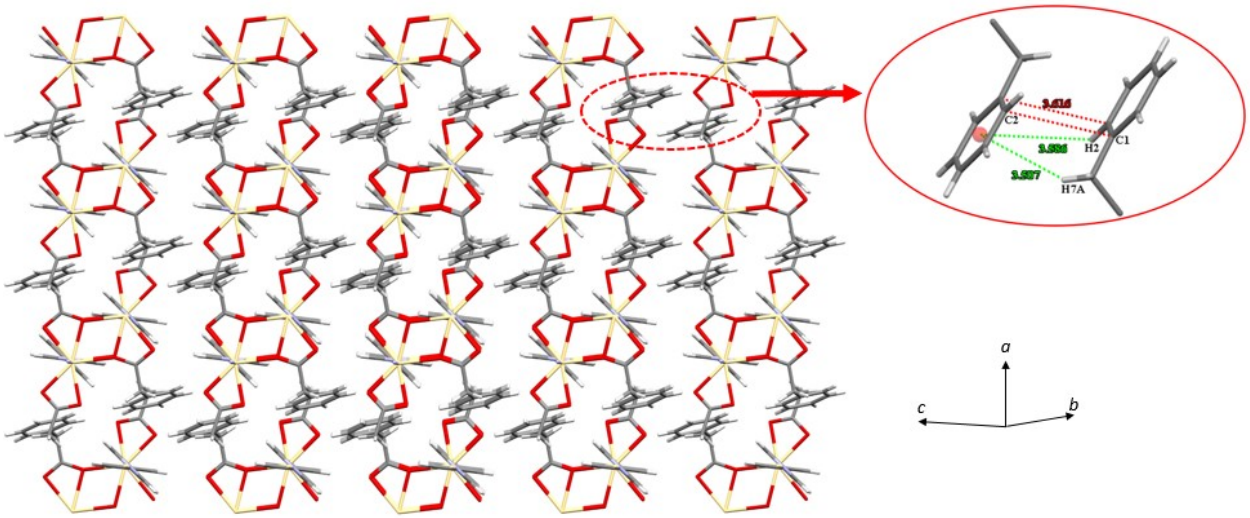

Figure S4. C-H/π (green dotted line) and off-set π-π stacking intermolecular interactions (red dotted line) in **2**.

a)

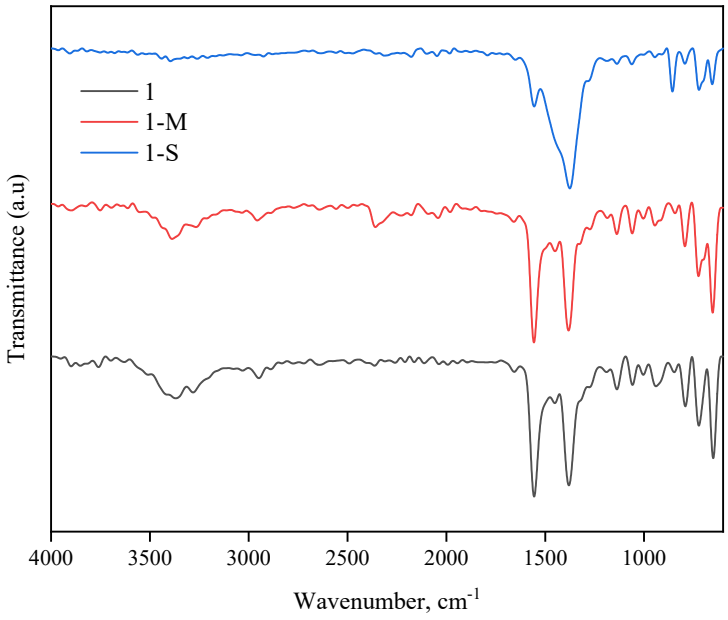

b)

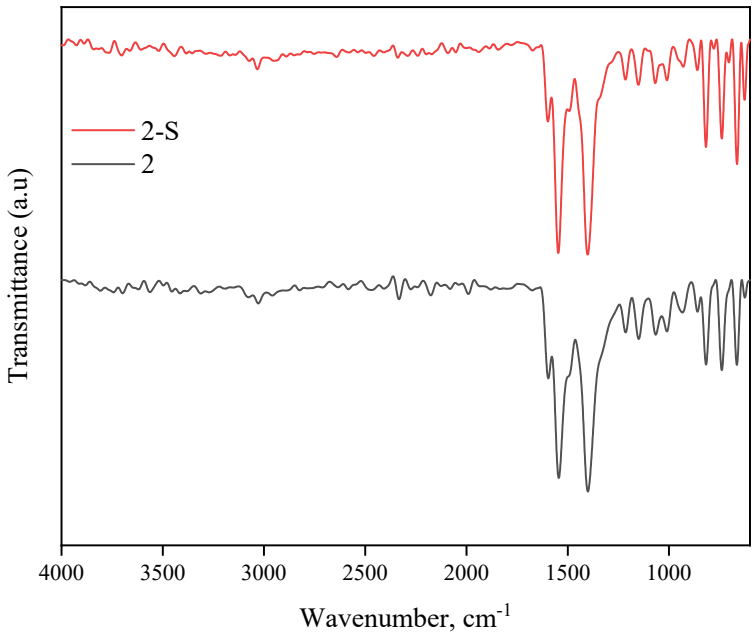

Figure S5. FT-IR spectra of compounds.

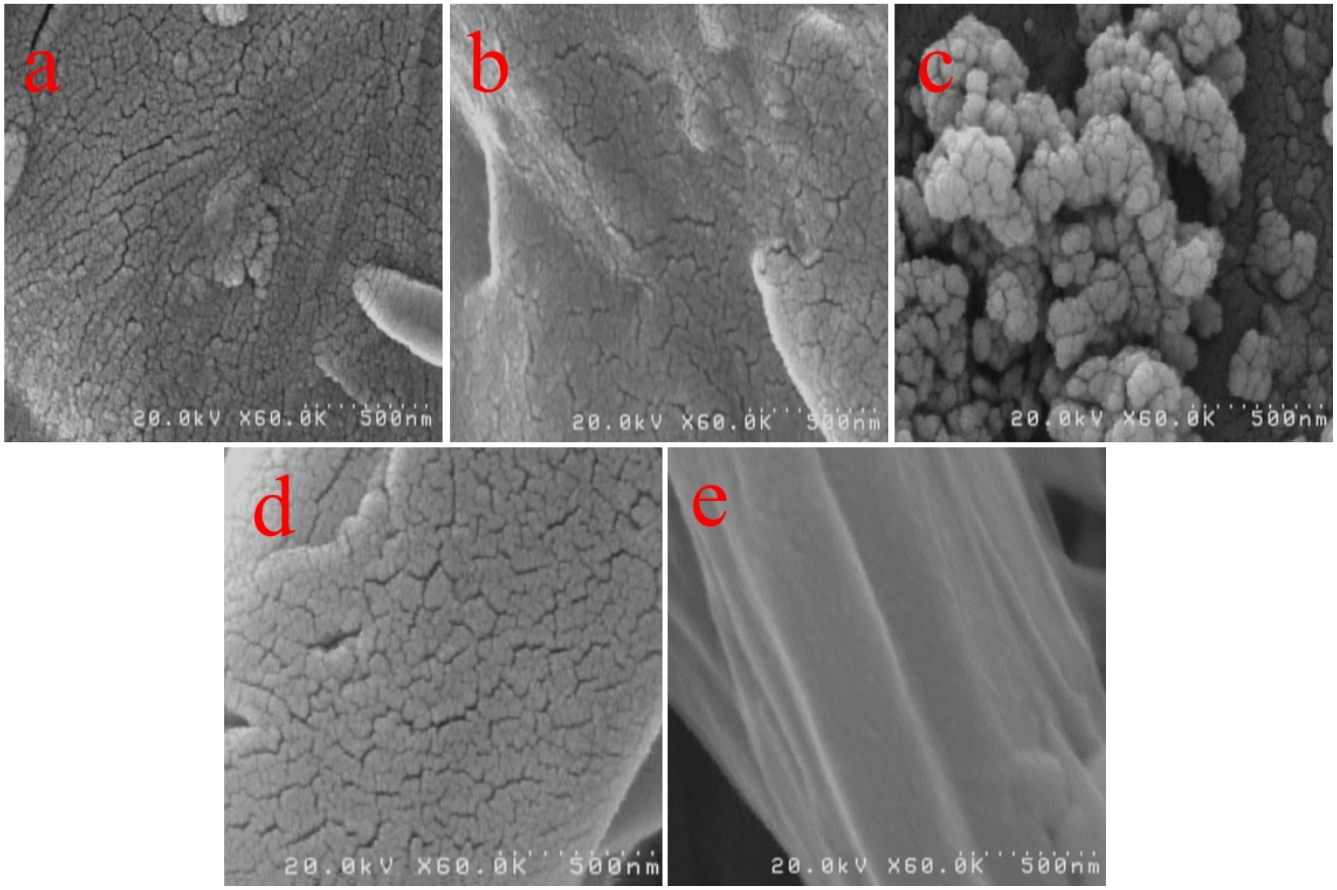

Figure S6. Magnified SEM images of **1** (a), **1-M** (b), **1-S** (c), **2** (d) and **2-S** (e).

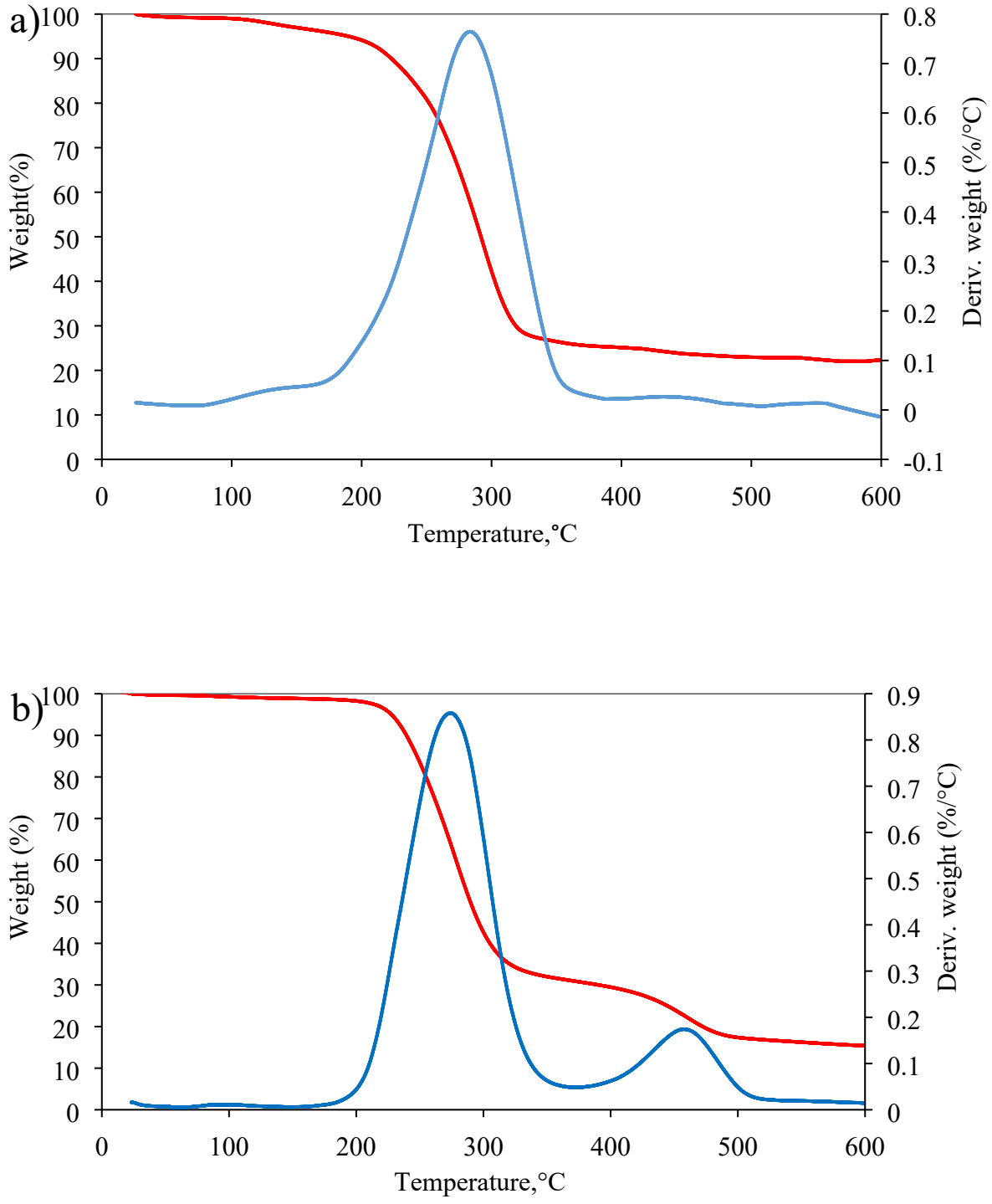

Figure S7. TGA-DTG curves of a) **1**, and b) **2**.

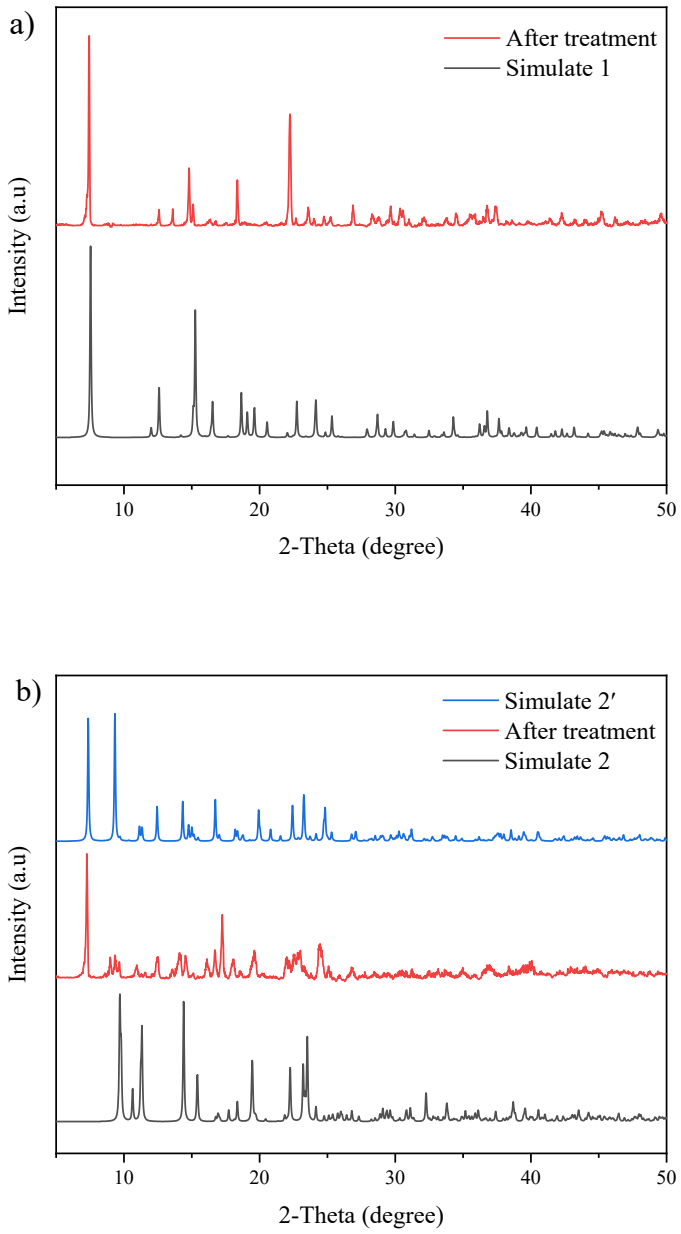

Figure S8. XRPD patterns of a) **1**, b) **2** after incubation for 24 hours. **2** after the treatment has been transformed by structural change into new phase (**2′**) with $[Cd_2(4,4'\text{-}Bpy)_2(Phac)_4]_n.0.25(H_2O)$ formula.

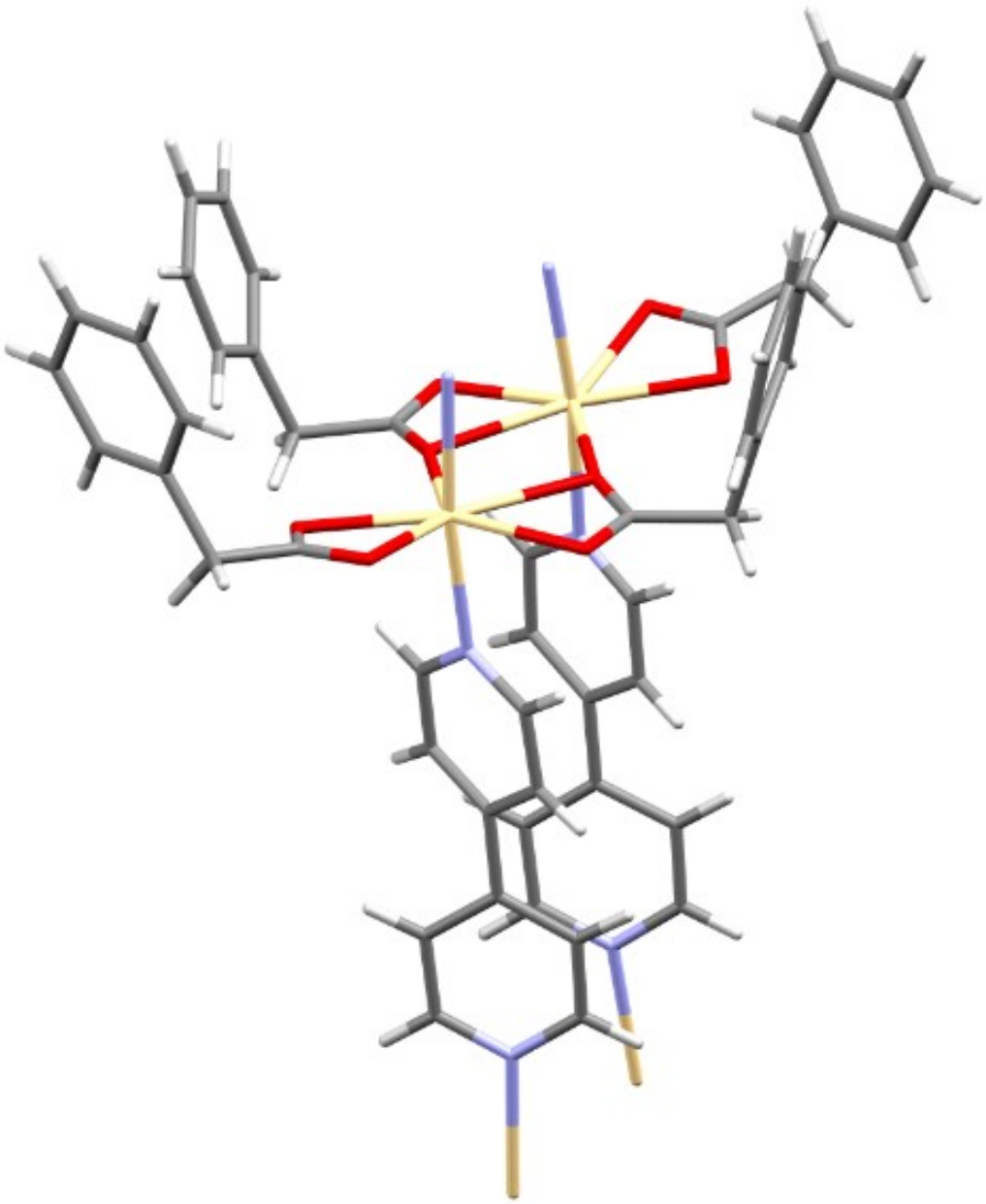

Figure S9. Fragment of the **2′** structure.

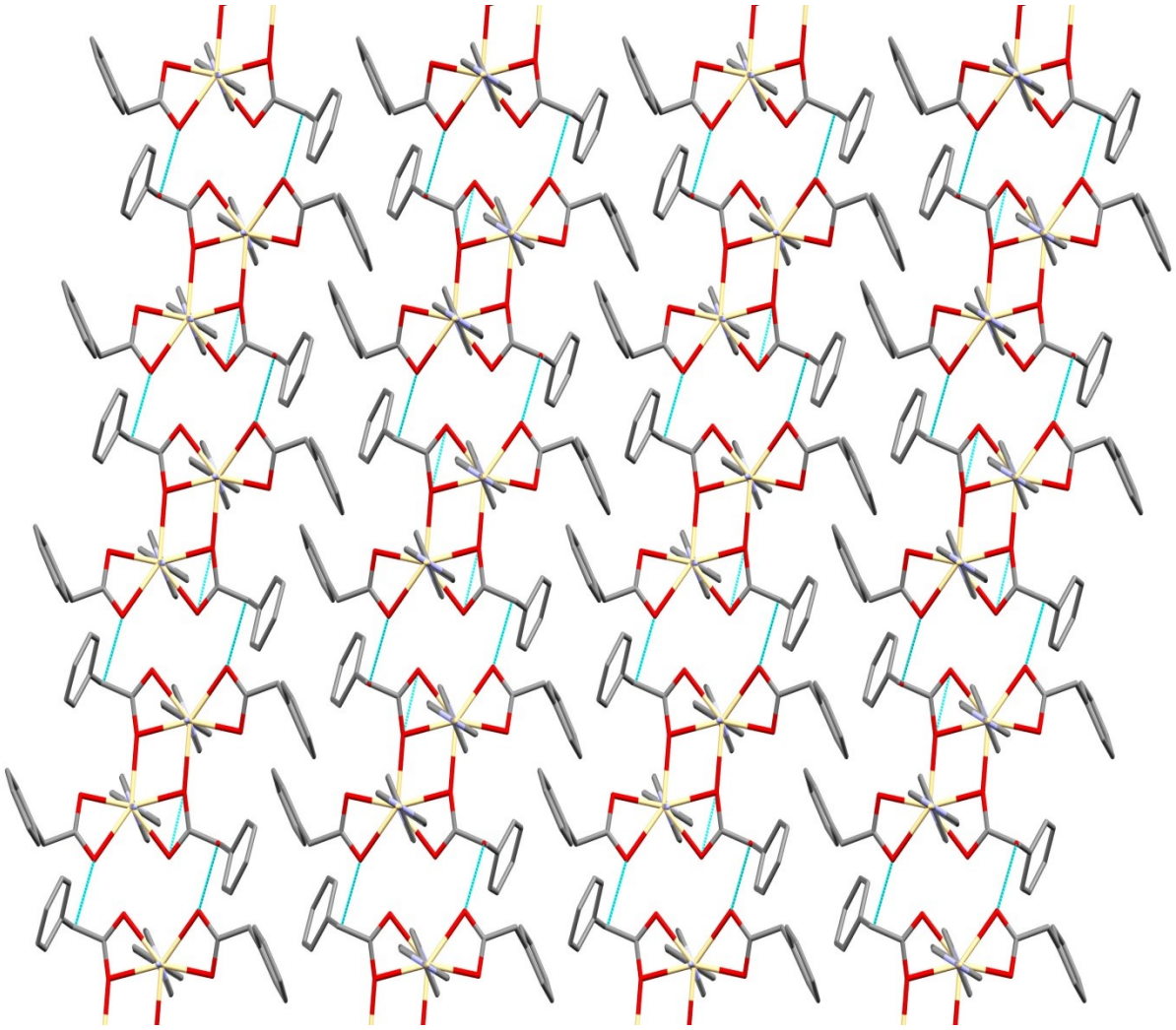

Figure S10. Replacement of phenylacetate ligand instead of acetate ligand in **2′** leads to network expansion through hydrogen bonds and more electrostatic interactions.

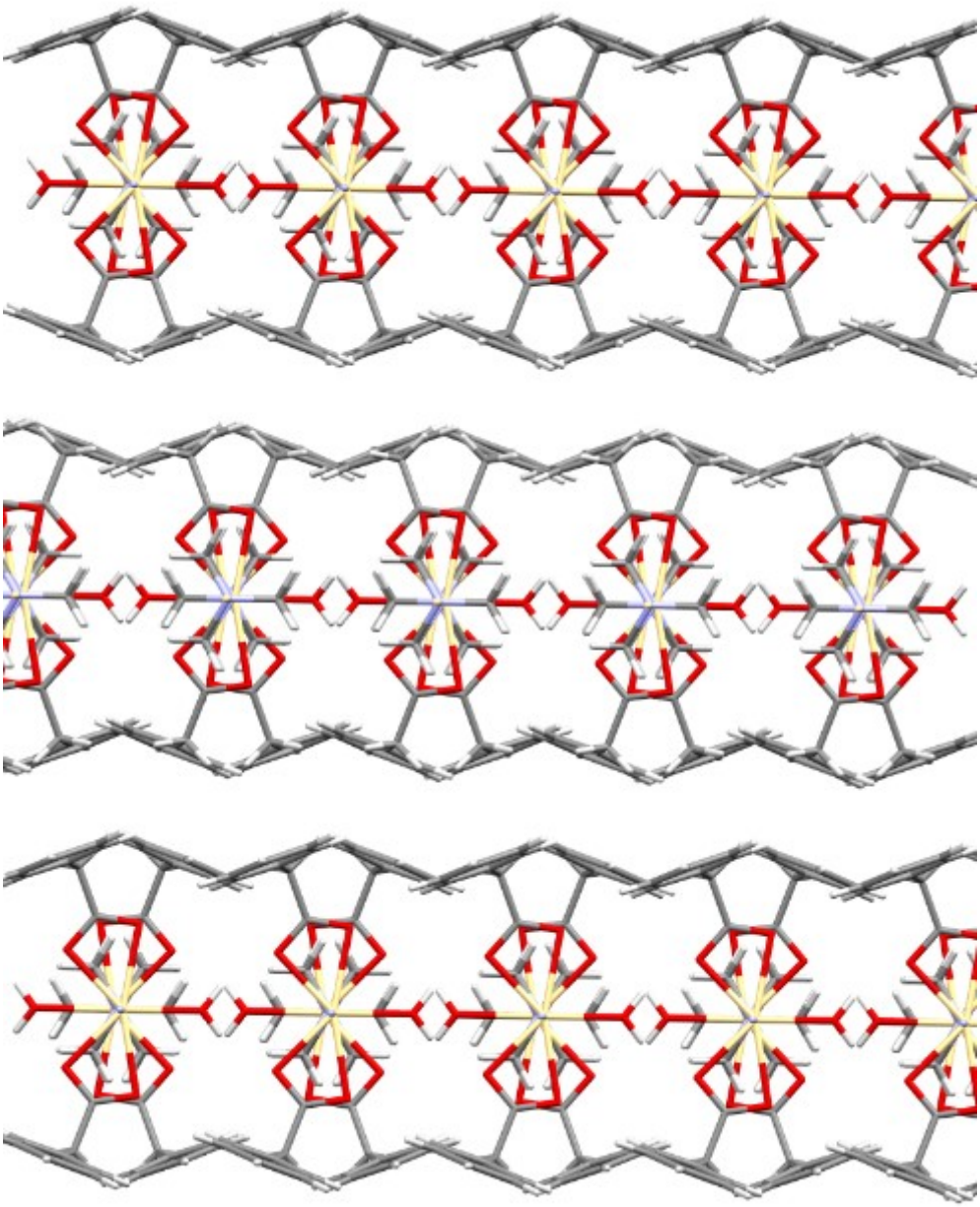

Figure S11. The shielding effect created around the central cadmium due to phenylacetate ligands in **1**.